THE BALTIC JOURNAL
OF ROAD AND BRIDGE ENGINEERING

ISSN 1822-427X / eISSN 1822-4288
2014 Volume 9(4): 283–296

EVALUATION OF STIFFNESS TO PREDICT RUTTING RESISTANCE OF HOT-MIX ASPHALT: A CANADIAN CASE STUDY

Md. Safiuddin[1]✉, Susan Louise Tighe[2], Ludomir Uzarowski[3]

[1]*Angelo del Zotto School of Construction Management, George Brown College, 146 Kendal Avenue, Toronto, M5T 2T9 Ontario, Canada*
[2]*Centre for Pavement and Transportation Technology, Dept of Civil and Environmental Engineering, University of Waterloo, 200 University Avenue West, Waterloo, N2L 3G1 Ontario, Canada*
[3]*Golder Associates Limited, 100 Scotia Court, Whitby, L1N 8Y6 Ontario, Canada*
E-mails: [1]msafiuddin@georgebrown.ca; [2]sltighe@uwaterloo.ca; [3]luzarowski@golder.com

Abstract. This paper investigates the relationship between the stiffness and rutting resistance of hot-mix asphalt. Ten different types of hot-mix asphalt were examined. The Superpave mix design method was utilized to produce nine mixes; the remaining mix was designed using the Marshall method. The asphalt mixes were tested for stiffness and rutting resistance under the Centre for Pavement and Transportation Technology research program at the University of Waterloo. The stiffness was determined by the laboratory resilient and dynamic moduli tests. The dynamic modulus test was conducted at six different loading frequencies and five different temperatures. The rutting test was executed by the Hamburg Wheel Rut Tester and the French Laboratory Rutting Tester to obtain rutting depth. The regression analysis was performed to examine the relationships of resilient and dynamic moduli with rutting depth. The results of the regression analysis revealed that resilient modulus did not correlate well with rutting depth. In contrast, dynamic modulus showed strong correlation with rutting depth for a number of loading frequencies and temperatures. The strong relationship was observed at the higher temperatures of +46.1 °C and +54.4 °C. Moreover, the relationship between dynamic modulus and rutting depth was better for lower loading cycles/wheel passes applied in the rutting test. It was also noticed that dynamic modulus exhibited a better relationship with rutting depth obtained from the French Laboratory Rutting Tester. The overall findings indicate that the dynamic moduli obtained at 0.1–1.0 Hz and +46.1–(+54.4) °C are useful to predict the rutting resistance of hot-mix asphalt.

Keywords: dynamic modulus, hot-mix asphalt, regression analysis, resilient modulus, rutting resistance, stiffness.

1. Introduction

Hot-Mix Asphalt (HMA) is a common pavement material in Canada. The main components of HMA are fine and coarse aggregates, and asphalt cement or binder. Both virgin mineral aggregates and recycled asphalt aggregates, such as Reclaimed or Recycled Asphalt Pavement (RAP) and Recycled Asphalt Shingles (RAS), are used in HMA (Tighe *et al.* 2007). Nowadays, the use of RAP in HMA as a partial replacement of virgin aggregates has become more prevalent in the pavement industry (Čygas *et al.* 2011; Swamy *et al.* 2011). In HMA mixes, the proportion of aggregates (virgin or virgin plus recycled) varies in the range of 84–90% by volume and the volume content of asphalt cement typically ranges from 3.0% to over 6.0% as described in *National Cooperative Highway Research Program (NCHRP) Report No. 673: A Manual for Design of Hot-Mix Asphalt with Commentary*. The HMA is also engineered to contain air and the volume of air voids is generally 3.0–5.0% as decpicted in *NCHRP Report No. 673*. Depending on the aggregate structure, HMA is classified as dense-graded, open-graded or uniformly-graded, and gap-graded or stone-mastic. It is extensively used in highways, airfields, parking lots, and port facilities in Canada.

The HMA is generally designed and used in flexible pavement to provide the desired service life with good resistance to permanent deformation under expected traffic loads. The nature of aggregate gradation (fine or coarse) affects the permanent deformation of asphalt in pavement (Khedr, Breakah 2011). Therefore, the gradation design of aggregates is optimized for HMA to improve its resistance to permanent deformation such as rutting (Sivilevičius *et al.* 2011). An ideal HMA mix is highly resistant to permanent deformation. However, a HMA mix undergoes rutting when it is not properly designed and placed. In

doi:10.3846/bjrbe.2014.35
http://www.bjrbe.vgtu.lt

service conditions, a HMA pavement exhibits significant rutting due to repeated traffic loading (Erlingsson 2012). The HMA is a time-dependent and stress-dependent material; it exhibits elastic, plastic, viscoelastic, and viscoplastic responses when subjected to the repeated loading (Ahmad *et al.* 2011). The repeated loading causes permanent strains, which must be considered in assessing the rutting resistance of HMA.

Rutting is typically a surface depression, which occurs in the wheel path of the HMA pavement. This is a kind of permanent deformation in the pavement caused by the traffic loads. Generally, the rutting occurs because of insufficient compaction during pavement construction, surface wear by chains and studded tires, overweight traffic, inadequate stability of asphalt, and deficient structural capacity of pavement (Coleri *et al.* 2013; Uzarowski 2006). According to *NCHRP Guide for Mehanistic-Empirical Design of New and Rehabilitated Pavement Structures*, the rutting of HMA is classified as vertical compression and depression with shear upheavals. The vertical compression rutting occurs in the form of a depression without any accompanying hump due to one-dimensional densification of HMA including excessive air voids or lacking adequate compaction (Coleri *et al.* 2013). On the contrary, the rutting in the form of a depression with accompanying shear upheavals occurs because of the lateral flow of HMA; the lateral flow is usually observed in the top 100 mm of the pavement surface (Uzarowski 2006). In most cases, the rutting in HMA pavement is caused by a combination of densification and shear-related deformation (Hu *et al.* 2011).

The rutting of HMA is linked with stiffness over a diverse range of climatic and traffic conditions (Ahmad *et al.* 2011; Goh *et al.* 2011; Tighe *et al.* 2007). The mix variables such as aggregate type, size and gradation, asphalt cement content, air void content, and mineral filler content were found to affect the rutting resistance of HMA mixes by influencing their stiffness (Al-Khateeb *et al.* 2013; Al-Suhaibani *et al.* 1992; Blazejowski, Dolzycki 2014; Neubauer, Partl 2004; Roy *et al.* 2013). Most of the aforementioned studies emphasized the effects of different factors on both the stiffness and rutting resistance of HMA mixture. However, none of the above studies highlighted the relationship between stiffness and rutting resistance for the traffic and climatic conditions of Canada. This research is directed at investigating the relationship between stiffness and rutting resistance of different typical Ontario HMA mixes. Ten different HMA mixes were produced and tested for stiffness and rutting resistance. The dynamic and resilient moduli tests were carried out to determine the stiffness. The rutting depth was measured by the Hamburg Wheel Rut Tester (HWRT) and the French Laboratory Rutting Tester (FLRT) to evaluate the rutting resistance. Based on the overall test results, the regression analysis was carried out to examine the nature of the relationship between HWRT/FLRT rutting depth and resilient/dynamic modulus. The results of regression analysis revealed that no good relationship exists between resilient modulus and rutting depth. In contrast, dynamic modulus showed excellent and good relationships with rutting depth for a number of loading frequencies and temperatures. The excellent relationships were observed for the higher temperatures of +46.1 °C and +54.4 °C. In all of these cases, the strength of the relationships was better for the lower loading cycles/wheel passes used in FLRT and HWRT tests. It was also observed that dynamic modulus showed a better relationship with rutting depth obtained from the FLRT, as compared with the HWRT.

2. Scope and objective

The research was carried out to determine the stiffness and rutting resistance of different HMA mixes. Ten typical Ontario HMA mixes were produced and tested. The resilient and dynamic moduli tests were performed to examine stiffness whereas the HWRT and FLRT tests were conducted to determine rutting resistance with respect to rutting depth. The regression analysis was conducted to examine the relationship between stiffness and rutting depth for different loading frequencies and temperatures. The objective of finding such relationship was to predict the rutting resistance of HMA mixes from their stiffness. When they are well-correlated, the stiffness of an HMA mix is useful to estimate its rutting resistance. Moreover, this research implies that the type of test as well as the test condition significantly influences the relationship between the stiffness and rutting resistance of HMA.

3. Experimental procedure

3.1. Design and preparation of HMA mixes

In total, ten HMA mixes were produced. A conventional Hot Laid 3 (HL3) dense-graded Marshall surface course mix, two Stone-Mastic Asphalt (SMA) surface course mixes, and two dense-graded Superpave (SP) binder course mixes were produced. In addition, five dense-graded SP binder course mixes with RAS and/or RAP including a control mix (without RAP and RAS) were produced. The constituent materials and compositions of different HMA mixes are shown in Table 1. Two dominant nominal max sizes of 12.50 mm and 19.00 mm were considered to design the aggregate structure. The gradation of aggregate blend for different HMA mixes is provided in Table 2.

The HL3 asphalt mix was designed using the Marshall methodology to meet the requirements of *Ontario Provincial Standard Specifications (OPSS) 1150*. The HL3 mix is a typical dense-graded Marshall surface course mix with a max aggregate size of 16.0 mm used in Ontario on low to medium volume roads. It is a relatively low-cost mix, which typically contains natural aggregates. The *OPSS 1150* specifications require that there must not be less than 5.0% asphalt cement in the mix. The HL3 mix (Mix 1) used in this research met the specified gradation, volumetric, stability and flow requirements.

The SMA and SP asphalt mixes were designed using the Asphalt Institute Superpave mix design method described in *Superpave, Superpave Mix Design, Superpave Series No. 2 (SP 2)* to meet the requirements of *OPSS 1151*.

Table 1. Constituent materials and composition of different HMA mixes

Type of asphalt mix		Material	Aggregate composition, %	Asphalt mix composition, %
Surface course mixes	Mix 1: HL3	Crushed gravel (coarse aggregate)	40.00	37.88
		Asphalt sand (fine aggregate)	45.00	42.62
		Screenings (fine aggregate)	15.00	14.20
		New asphalt cement (PG 58-28)	–	5.30
	Mix 2: SMA1*	Crushed rock (coarse aggregate)	79.00	74.50
		Manufactured sand (fine aggregate)	13.00	12.26
		Mineral filler	8.00	7.54
		Cellulose fibre (additive)	–	0.30
		New asphalt cement (PG 70-28)	–	5.70
	Mix 3: SMA2*	Crushed rock (coarse aggregate)	79.00	74.50
		Manufactured sand (fine aggregate)	13.00	12.26
		Mineral filler	8.00	7.54
		Cellulose fibre (additive)	–	0.30
		New asphalt cement (PG 70-28)	–	5.70
Binder course mixes	Mix 4: SP19D	Crushed rock (coarse aggregate)	39.00	37.30
		Manufactured sand (fine aggregate)	51.00	48.78
		Screenings (fine aggregate)	10.00	9.57
		New asphalt cement (PG 64-28)	–	4.35
	Mix 5: SP19E	Crushed rock (coarse aggregate)	63.00	60.10
		High stability sand (fine aggregate)	37.00	35.30
		New asphalt cement (PG 70-28)	–	4.60
	Mix 6: SP19C	Crushed rock (coarse aggregate)	50.50	48.18
		Manufactured sand (fine aggregate)	36.50	34.82
		Screenings (fine aggregate)	13.00	12.40
		New asphalt cement (PG 58-28)	–	4.60
	Mix 7: SP19C, 20% RAP	Crushed rock (coarse aggregate)	39.70	37.87
		Manufactured sand (fine aggregate)	29.30	27.95
		¼ in. chips (fine aggregate)	11.00	10.50
		RAP	20.00	19.08
		New asphalt cement (PG 52-28)	–	3.80
		Asphalt cement from RAP	–	0.80
	Mix 8: SP19C, 20% RAP, 1.4% RAS	Crushed rock (coarse aggregate)	39.60	37.78
		Manufactured sand (fine aggregate)	29.00	27.67
		¼ in chips (fine aggregate)	10.00	9.54
		RAP	20.00	19.08
		RAS	1.40	1.33
		New asphalt cement (PG 52-34)	–	3.41
		Asphalt cement from RAS	–	0.42
		Asphalt cement from RAP	–	0.77
	Mix 9: SP19C, 20% RAP, 3% RAS	Crushed rock (coarse aggregate)	42.00	40.07
		Manufactured sand (fine aggregate)	21.00	20.03
		Screenings (fine aggregate)	15.00	14.31
		RAP	19.00	18.13
		RAS	3.00	2.86
		New asphalt cement (PG 58-28)	–	2.61
		Asphalt cement from RAS	–	0.90
		Asphalt cement from RAP	–	1.09
	Mix 10: SP19C, 3% RAS	Crushed rock (coarse aggregate)	51.00	48.66
		Manufactured sand (fine aggregate)	21.00	20.03
		Screenings (fine aggregate)	25.00	23.85
		RAS	3.00	2.86
		New asphalt cement (PG 58-28)	–	3.70
		Asphalt cement from RAS	–	0.90

*aggregate gradation is different.

Table 2. Gradation of aggregate blend for different HMA mixes

Asphalt mix	Percent passing										
	26.50 mm	19.00 mm	12.50 mm	9.50 mm	4.75 mm	2.36 mm	1.18 mm	600 μm	300 μm	150 μm	75 μm
Mix 1	100	100	96.0	86.0	60.0	50.7	40.9	28.8	13.3	5.7	3.7
Mix 2	100	100	98.8	71.1	25.4	21.3	17.5	14.8	13.0	10.8	9.1
Mix 3	100	100	90.0	65.7	25.0	18.3	14.3	13.0	10.6	9.0	8.0
Mix 4	100	97.2	77.9	68.2	60.2	44.6	29.7	18.8	9.9	5.3	4.2
Mix 5	100	97.0	80.2	63.2	38.0	33.4	22.5	14.4	8.7	5.2	3.8
Mix 6	100	95.6	81.5	67.5	49.9	39.6	27.0	17.3	10.6	5.9	4.2
Mix 7	100	96.8	86.5	73.0	50.1	36.5	25.5	16.8	10.1	5.1	3.3
Mix 8	100	96.8	86.5	73.0	50.3	37.3	26.2	17.3	10.5	5.5	3.6
Mix 9	100	96.3	84.4	70.7	49.4	38.9	27.3	18.7	12.3	7.4	5.2
Mix 10	100	95.2	80.0	66.0	47.7	37.0	24.5	16.1	10.7	6.8	4.9

The SMA is a gap-graded premium surface course mix with enhanced rutting resistance. It is used in Ontario on high volume roads, mainly freeways and very busy major arterial city roads for traffic categories *D* (10 mln ESALs to 30 mln ESALs) and *E* (more than 30 mln ESALs). Only 100% crushed and quarried coarse and fine aggregates are used in SMA mixes. In the present study, both the SMA1 (Mix 2) and SMA2 (Mix 3) mixes were designed for category *E* roads and both met the specified gradation and volumetric requirements. The gradations of both mixes were very close and the asphalt cement contents were the same.

The SP19 mix is typically used as a binder course in Ontario. This mix is designed for traffic category *A*, *B*, *C*, *D* and *E* (<0.3 mln ESALs to >30 mln ESALs). In the present study, the SP19D mix (Mix 4) was designed for category *D* (10 mln ESALs to <30 mln ESALs) whereas the SP19E mix (Mix 5) was designed for category *E* (≥30 mln ESALs) traffic loading. The SP19C mixes (Mixes 6–10) were designed for category *C* (3 mln ESALs to <10 mln ESALs) traffic loading. All SP mixes met the Superpave gyratory compaction requirements at the $N_{initial}$ and N_{max} number of gyrations. Also, all SP mixes met the gradation and volumetric requirements. In general, the SP19E mix was much coarser than the SP19C and SP19D mixes. The SP19E mix had significantly higher asphalt cement content than the SP19D mix. However, the SP19C and SP19E mixes had the same asphalt cement.

Coarse and fine aggregates, performance-graded asphalt cement, mineral filler (optional), and cellulose fiber (optional additive) were used to prepare the HMA mixes. The asphalt cement was selected based on the climatic (temperature) and loading (traffic) conditions that the HMA pavement was expected to undergo. The mineral aggregates, asphalt cement, mineral filler, and additive (if any) were mixed thoroughly to produce the HMA mixes. Mixes 1–5 were obtained from the different paving projects in Ontario and delivered to the Golder Associates Limited (Golder) laboratory in Whitby, Ontario. The sample preparation for volumetric properties and rutting testing of these five HMA mixes was carried out in this laboratory. However, the sample preparation for stiffness testing of these asphalt mixes was performed in the Centre for Pavement and Transportation Technology (CPATT) laboratory at the University of Waterloo, Ontario, Canada. Mixes 6–10 were prepared and delivered to CPATT in Waterloo and École de Technologie Superieure (ETS) in Montreal by Miller Paving Limited, Markham, Ontario, Canada. The sample preparation for volumetric properties and stiffness testing of these HMA mixes was performed in the CPATT laboratory. The sample preparation for rutting testing of these asphalt mixes was carried out in the ETS laboratory.

The volumetric properties of different HMA mixes are presented in Table 3. The design air voids of the asphalt mixes were 4.0–4.2%. The design asphalt cement content was in the range of 4.35–5.70%. The dust-to-binder ratio differed in the range of 0.72–1.50%. In the course of the volumetric mix design, the asphalt mixes were conditioned in an oven according to the specified heating time and compaction temperature.

3.2. Fabrication of test specimens

The loose asphalt mixes were oven-conditioned following the specified heating time and compaction temperature before fabricating the test specimens. The conditioned asphalt mixes were compacted using a Superpave Gyratory Compactor (SGC) to produce Ø150×170H mm cylinders. Triplicate Ø150×50H mm cylinders were obtained by cutting one Ø150×170H mm cylinder for use in the resilient modulus test. Also, Ø100×150H mm cylinder specimens were cored from Ø150×170H mm cylinders for use in the dynamic modulus test. In the case of HWRT rutting test, Ø150×63H mm briquette specimens were prepared by cutting the Ø150×170H mm cylinders obtained in the SGC. Moreover, the conditioned asphalt mixes were compacted using a slab compactor to form 500L×180W×100H mm block specimens for use in the FLRT rutting test.

Table 3. Volumetric properties of different HMA mixes

Asphalt mix	Air voids	*VMA*, %	*VFA*, %	$\%G_{mm}$ at N_{ini}	$\%G_{mm}$ at N_{max}	*D*/*B* ratio	Marshall stability, N	Flow, 0.25 mm
Mix 1	4.0	15.5	74.2	NA	NA	NA	9,600	8.7
Mix 2	4.0	18.2	78.0	–	–	1.5	NA	NA
Mix 3	4.0	17.5	77.1	–	–	–	NA	NA
Mix 4	4.0	13.3	69.9	88.5	96.9	0.9	NA	NA
Mix 5	4.0	13.0	69.4	86.8	97.2	1.02	NA	NA
Mix 6	4.2	13.7	69.3	86.9	–	0.91	NA	NA
Mix 7	4.0	14.0	71.4	87.6	–	0.72	NA	NA
Mix 8	4.0	13.9	71.2	87.6	–	0.78	NA	NA
Mix 9	4.0	13.0	69.2	91.5	–	1.13	NA	NA
Mix 10	4.04	13.4	69.9	87.8	–	1.06	NA	NA

Note: D/*B* – dust-to-binder ratio; N_{ini} – initial gyrations; N_{max} – max gyrations; *VMA* – voids in the mineral aggregate; *VFA* – voids filled with asphalt; $\%G_{mm}$ – percent theoretical max specific gravity.

3.3. Laboratory testing

All asphalt mixes were tested for the dynamic modulus and rutting resistance. Mixes 6–10 were also tested for the resilient modulus.

3.3.1. Resilient modulus test

Resilient modulus is a measure for the stiffness of materials. It provides a means to analyze the stiffness of materials under different conditions. The resilient modulus of different HMA mixes was determined in accordance with the procedure given in *AASHTO TP31-1996: Standard Test Method for Determining the Resilient Modulus of Bituminous Mixtures by Indirect Tension Test*. The resilient modulus test was performed in the CPATT laboratory. Triplicate Ø150×50 mm cylinder specimens were used for each mix. The air void content of the specimens was 7±1.0%. The test temperature was +25.0 °C. The specimens were tested at two different orientations or diametrical positions. The second orientation involved rotating the specimen by 90°. For each orientation, the test was run three times for each asphalt mix. The loading sequence on the specimens consisted of a haversine pulse with a frequency of 1.0 Hz. The load was applied for a duration of 0.1 s followed by a rest period of 0.9 s at each loading cycle.

3.3.2. Dynamic modulus test

Dynamic modulus is defined as the ratio of stress to strain under vibratory conditions. It is a measure for the stiffness of materials. The dynamic modulus of different HMA mixes was determined according to the procedure given in *AASHTO TP62-2003 Standard Test Method for Determining Dynamic Modulus of Hot-Mix Asphalt Concrete Mixtures*. The dynamic modulus test was carried out in the CPATT laboratory. Triplicate Ø100×150H mm cylinder specimens were used in this test. The air void content of the specimens was 6±1% for the Mixes 1–5 and 7±1% for the Mixes 6–10. The test specimens were subjected to a repetitive, compressive, and sinusoidal load. Two linear variable differential transducers (LVDTs) were used to measure the deformation of test specimens. Each specimen was tested at six loading frequencies (0.1 Hz, 0.5 Hz, 1.0 Hz, 5.0 Hz, 10.0 Hz and 25 Hz) and five temperatures (–10.0 °C, +4.4 °C, +21.1 °C, +37.8 °C and +54.4 °C).

3.3.3. Rutting tests

Mixes 1–5 were tested by the HWRT. The details of the HWRT are described in Uzarowski *et al.* (2004, 2006, 2008). The HWRT rutting test was performed in the Golder laboratory. Two sets of specimens were used for each asphalt mix to carry out the test. Each set consisted of triplicate Ø150×63H mm briquette specimens. Solid rubber wheels (50 mm wide) were used and the load applied to the wheels was 710±1 N. The testing was performed in dry condition and the test temperature was +50 °C. The test was carried out for up to 20 000 passes of the wheels. The wheels made approx 50 passes per minute (loading frequency – 0.83 Hz). The loading time for 1 pass was 0.21 s. Therefore, the total loading time for the entire test (20 000 passes) was 4200 s (70 min). The permanent deformation versus the number of passes results were gathered by a data acquisition system.

Mixes 6–10 were tested by the FLRT. The details of the FLRT are depicted in Uzarowski *et al.* (2004). Each asphalt mix was tested at durations of 100, 300, 1000, 3000, 10 000, and 30 000 cycles. Duplicate 500L×180W×100H mm block specimens were used for each mix. The repetitive load was applied on the block specimens by passing a pneumatic tire (400 mm diameter and 80 mm wide) at a frequency of 1 Hz. The pressure of the tire was set at 600±30 kPa and the load applied was 5000±50 N. The test temperature was +60 °C. Such testing conditions were followed to simulate the same loading conditions that the asphalt mixes experience in the field during a hot summer day under a heavy traffic load.

4. Test results and discussion

4.1. Resilient modulus test results

The results of the resilient modulus test are given in Table 4. The resilient modulus values were obtained at the loading frequency of 1 Hz and testing temperature of +25 °C. Table 4 reveals that the resilient modulus depended upon the orientation of the specimens during testing. The average resilient modulus varied in the range of 0.597–1.583 GPa. Mix 6 (SP19C) was found to have the highest resilient modulus. The lowest resilient modulus was obtained for Mix 10. The resilient modulus was 1.25–1.60% lower than the dynamic modulus when compared at the similar testing conditions (loading frequency: 1 Hz; testing temperature: +21.1 °C/+25 °C). This suggests that the resilient modulus test is less efficient than the dynamic modulus test in characterizing the stiffness of HMA. A similar finding was reported by Loulizi *et al.* (2006).

4.2. Dynamic modulus test results

The detailed results of the dynamic modulus test are presented in Table 5. The dynamic modulus varied in a wide range of 0.244–30.403 GPa. These dynamic modulus values were obtained for five different temperatures (–10.0 °C, +4.4 °C, +21.1 °C, +37.8 °C and +54.4 °C) and six different loading frequencies (0.1 Hz, 0.5 Hz, 1.0 Hz, 5.0 Hz, 10.0 Hz and 25 Hz). Mix 4 provided the highest dynamic modulus. The lowest dynamic modulus was obtained for Mix 8. The overall results obtained reveal that the dynamic modulus values depend on both loading frequencies and temperatures. A higher dynamic modulus was obtained for a greater loading frequency whereas a lower dynamic modulus was achieved at a higher testing temperature (Table 5). Similar effects of loading frequency and testing temperature were reported from earlier research (Bhattacharjee *et al.* 2008; Khan, Kamal 2012; Yu, Shen 2012).

Table 4. Resilient modulus test results for different HMA mixes

Asphalt mix	Resilient modulus, GPa		
	Primary position (0° orientation)	Secondary position (90° orientation)	Average
Mix 6	1.500	1.666	1.583
Mix 7	1.330	1.357	1.344
Mix 8	1.339	1.205	1.272
Mix 9	0.816	0.606	0.711
Mix 10	0.617	0.576	0.597

Table 5. Dynamic modulus test results for different HMA mixes

Asphalt mix	Frequency, Hz	Average dynamic modulus, GPa					
		−10.0 °C	4.4 °C	21.1 °C	37.8 °C	46.1 °C	54.4 °C
Mix 1	0.1	12.462	5.905	1.924	0.876	–	0.543
	0.5	17.025	8.411	2.903	1.139	–	0.723
	1.0	19.464	8.970	3.567	1.324	–	0.789
	5.0	23.759	14.155	5.632	2.002	–	1.063
	10.0	26.141	15.782	6.725	2.532	–	1.241
	25.0	29.036	18.234	8.517	3.678	–	1.772
Mix 2	0.1	13.671	7.409	2.052	0.858	–	0.661
	0.5	16.198	10.030	3.116	1.124	–	0.698
	1.0	19.474	11.374	3.814	1.313	–	0.743
	5.0	22.299	14.503	6.006	2.018	–	0.940
	10.0	26.149	15.864	7.122	2.577	–	1.135
	25.0	28.329	17.782	8.992	3.788	–	1.635
Mix 3	0.1	8.277	4.029	1.232	0.750	–	0.583
	0.5	12.003	6.336	1.868	0.902	–	0.684
	1.0	13.744	7.607	2.287	1.003	–	0.734
	5.0	17.533	10.777	3.689	1.406	–	0.903
	10.0	19.329	12.317	4.512	1.719	–	1.043
	25.0	21.881	14.304	5.971	2.476	–	1.401

Continued Table 5

Mix 4	0.1	14.549	9.637	3.308	1.547	–	1.036
	0.5	18.948	12.641	4.765	2.128	–	1.225
	1.0	21.139	14.062	5.656	2.509	–	1.349
	5.0	25.117	17.367	8.079	3.780	–	1.807
	10.0	27.300	18.869	9.209	4.534	–	2.165
	25.0	30.403	21.183	11.078	5.899	–	2.975
Mix 5	0.1	11.332	6.810	2.272	1.370	–	1.088
	0.5	15.866	10.040	3.607	1.726	–	1.176
	1.0	18.039	11.730	4.506	1.957	–	1.242
	5.0	22.305	15.563	7.151	2.817	–	1.484
	10.0	24.465	17.316	8.545	3.458	–	1.696
	25.0	27.417	19.914	10.709	4.848	–	2.234
Mix 6	0.1	11.628	6.275	0.978	0.323	0.278	–
	0.5	15.492	9.252	1.796	0.427	0.333	–
	1.0	17.084	10.633	2.514	0.520	0.381	–
	5.0	20.573	13.997	4.681	0.968	0.587	–
	10.0	21.423	15.296	5.667	1.315	0.818	–
	25.0	23.166	17.206	7.376	2.034	1.249	–
Mix 7	0.1	13.044	5.734	0.769	0.356	0.341	–
	0.5	16.607	8.459	1.383	0.451	0.398	–
	1.0	18.093	9.760	1.851	0.532	0.451	–
	5.0	21.465	12.913	4.033	0.935	0.714	–
	10.0	22.205	14.165	4.531	1.222	0.999	–
	25.0	24.203	16.022	6.086	1.853	1.462	–
Mix 8	0.1	8.000	3.726	0.842	0.338	0.244	–
	0.5	10.911	5.623	1.402	0.451	0.303	–
	1.0	12.192	6.571	1.778	0.540	0.358	–
	5.0	15.125	9.104	3.185	0.925	0.559	–
	10.0	15.965	10.061	3.868	1.201	0.725	–
	25.0	17.624	11.534	5.028	1.800	1.179	–
Mix 9	0.1	5.125	1.239	0.448	0.282	0.257	–
	0.5	7.218	1.914	0.616	0.351	0.300	–
	1.0	8.306	2.405	0.744	0.407	0.343	–
	5.0	11.292	4.202	1.582	0.627	0.481	–
	10.0	12.125	4.284	1.504	0.781	0.606	–
	25.0	13.971	5.422	1.991	1.102	0.922	–
Mix 10	0.1	3.068	0.813	0.480	0.326	0.288	–
	0.5	4.836	1.217	0.633	0.376	0.318	–
	1.0	5.785	1.496	0.746	0.421	0.361	–
	5.0	8.573	2.815	1.148	0.605	0.482	–
	10.0	9.272	2.989	1.386	0.737	0.597	–
	25.0	11.012	3.829	1.805	1.030	0.944	–

4.3. Rutting test results

4.3.1. HWRT rutting results

The rutting resistance of the asphalt mixes was evaluated based on the deformation after 10 000, 15 000 and 20 000 passes. The results of the HWRT rutting test for Mixes 1–5 are given in Table 6. The percent rutting depth was calculated based on the original thickness (63 mm) of the specimens. The rutting rate for 10 000 passes was more than the rutting rate for 20 000 passes. This is because the densification of the asphalt mixes was relatively high at the beginning of the test. Nevertheless, the percent rutting depth for all asphalt mixes was lower than the max allowable criteria after 20 000 passes, except for the HL3 mix (Mix 1), which is known to be more susceptible to rutting. According to Uzarowski *et al.* (2004, 2006), the max allowable rutting depth after 20 000 passes is 1.90 mm (3% for 63 mm thick specimen) for surface course and 1.82 mm (2.9% for 63 mm thick specimen) for base course in the case of Class I traffic loading (extremely heavy, slow, and stopping traffic). However, all asphalt mixes passed the rutting criteria for Class II traffic loading. Moreover, the rutting depth was significantly below the max allowable limit specified by the Texas Department of Transportation (*TxDOT*). According to *TxDOT HWRT Specifications*, the max allowable rutting depth is 12.50 mm (19.8% for 63 mm thick specimen). This criterion is for the HWRT test conducted using a steel wheel in wet condition. In the present study, the HWRT test was performed using a rubber wheel in dry condition. However, the test temperature was the same as mentioned in *TxDOT HWRT Specifications*.

4.3.2. FLRT rutting results

In the FLRT test, the rutting resistance of the asphalt mixes was evaluated based on the deformation after 100, 300, 1000, 3000, 10 000 and 30 000 cycles. The results of the FLRT rutting test for the five SP19C mixes (Mixes 6–10) are provided in Table 7. The percent rutting depth was calculated based on the original thickness (100 mm) of the specimens. It is obvious from Table 7 that the FLRT rutting rate was relatively high at lower cycles. As noted, this is similar to the HWRT rutting results.

The overall FLRT rutting was very small when compared with the max allowable rutting depth. The FLRT rutting depth of the HMA mixes designed for heavily trafficked pavements is not expected to be more than 10 mm or 20% of the initial thickness (50 mm thick specimen) after 3000 cycles for surface course and 10 mm or 10% of the initial thickness (100 mm thick specimen) after 30 000 cycles for base course (Uzarowski *et al.* 2004). In the present study, the FLRT rutting depth of the asphalt Mixes 6–10 (designed for base course) after 30 000 cycles

Table 6. HWRT rutting results for different HMA mixes

Asphalt mix	Specimens set	Rutting depth, %		
		After 10 000 passes	After 15 000 passes	After 20 000 passes
Mix 1	A	2.86	3.17	3.43
	B	3.17	3.75	4.29
	Average	3.02	3.46	3.86
Mix 2	A	2.03	2.16	2.25
	B	2.13	2.29	2.38
	Average	2.08	2.23	2.32
Mix 3	A	2.41	2.64	2.79
	B	2.29	2.51	2.64
	Average	2.35	2.58	2.72
Mix 4	A	1.37	1.56	1.65
	B	1.52	1.65	1.78
	Average	1.45	1.61	1.72
Mix 5	A	1.94	2.19	2.38
	B	1.65	1.81	1.91
	Average	1.80	2.00	2.15

Table 7. FLRT rutting results for different HMA mixes

Asphalt mix	Specimen	Rutting depth, %					
		After 100 cycles	After 300 cycles	After 1000 cycles	After 3000 cycles	After 10 000 cycles	After 30 000 cycles
Mix 6	A	1.94	2.24	2.86	3.35	3.90	3.88
	B	1.78	2.24	2.74	3.13	3.76	3.95
	Average	1.86	2.24	2.80	3.24	3.83	3.92
Mix 7	A	2.54	3.34	3.77	4.28	5.02	5.31
	B	2.65	3.34	3.80	4.31	5.08	5.48
	Average	2.60	3.34	3.79	4.30	5.05	5.40
Mix 8	A	1.94	2.14	2.86	3.33	3.84	4.08
	B	1.66	2.14	2.52	3.05	3.55	3.77
	Average	1.80	2.14	2.69	3.19	3.70	3.93
Mix 9	A	1.24	1.49	1.99	2.41	2.98	4.00
	B	1.29	1.59	2.01	2.53	3.20	4.27
	Average	1.27	1.54	2.00	2.47	3.09	4.14
Mix 10	A	1.60	1.96	2.36	2.88	3.60	4.31
	B	1.36	1.66	2.13	2.61	3.29	4.16
	Average	1.48	1.81	2.25	2.75	3.45	4.24

varied in the range of 3.92–5.40%, which is significantly below the max allowable limit of 10%.

4.4. Relationship between dynamic modulus and rutting depth

The dynamic modulus values were obtained for all ten asphalt mixes. The HWRT rutting depth was measured for the HL3, SMA1, SMA2, SP19D, and SP19E mixes (Mixes 1–5) whereas the FLRT rutting depth was obtained for the five SP19C mixes (Mixes 6–10). The relationship of the dynamic modulus with both the HWRT and FLRT rutting depths was examined using regression analysis. The goodness of the relationship was determined based on the criteria given in Table 8. The characteristics of the best-fit relationships are shown in Tables 9 and 10.

The relationship between dynamic modulus of elasticity and rutting depth varied with the test temperature and loading frequency. The relationship of dynamic modulus with the HWRT rutting depth was very poor to poor for all loading frequencies (0.1–25.0 Hz) at −10.0 °C (Table 9). The excellent relationship for all HWRT wheel passes was attained at 0.1 Hz and +54.4 °C (Fig. 1). In this case, the best-fit lines were polynomial with a coefficient of determination in the range of 0.927–0.951. At +54.4 °C, a strong relationship was also observed for 0.5 Hz up to 15 000 wheel passes; the relationship was fair to good for the other loading frequencies and testing temperatures (Table 9). In

Table 8. Criteria for goodness of statistical relationship (Tran, Hall 2005)

Goodness of fit (*GF*)	Coefficient of determination, *CD*, R^2
Excellent (*E*)	≥0.90
Good (*G*)	0.70–0.89
Fair (*F*)	0.40–0.69
Poor (*P*)	0.20–0.39
Very poor (*VP*)	≤0.19

Table 9. Relationship between stiffness and HWRT rutting depth

Test conditions				Nature of relationship between DM and HWRT rutting depth								
DM stiffness test		HWRT rutting test		10 000 Passes			15 000 Passes			20 000 Passes		
f, Hz	*T*, °C	*f*, Hz	*T*, °C	*BFL*	*CD*	*GF*	*BFL*	*CD*	*GF*	*BFL*	*CD*	*GF*
0.1	−10.0	0.83	+50.0	*PN*	0.279	*P*	*PN*	0.280	*P*	*PN*	0.279	*P*
	+4.4			*PN*	0.564	*F*	*EP*	0.532	*F*	*EP*	0.491	*F*
	+21.1			*EP*	0.579	*F*	*EP*	0.527	*F*	*EP*	0.468	*F*
	+37.8			*EP*	0.697	*G*	*EP*	0.628	*F*	*EP*	0.556	*F*
	+54.4			*PN*	0.951	*E*	*PN*	0.944	*E*	*PN*	0.927	*E*
0.5	−10.0	0.83	+50.0	*PN*	0.204	*P*	*PN*	0.165	*VP*	*PN*	0.134	*VP*
	+4.4			*PN*	0.635	*F*	*PN*	0.585	*F*	*PN*	0.531	*F*
	+21.1			*EP*	0.589	*F*	*EP*	0.537	*F*	*EP*	0.475	*F*
	+37.8			*EP*	0.698	*G*	*EP*	0.629	*F*	*EP*	0.557	*F*
	+54.4			*PN*	0.792	*G*	*PN*	0.737	*G*	*PN*	0.690	*F*
1.0	−10.0	0.83	+50.0	*PN*	0.172	*VP*	*PN*	0.149	*VP*	*PN*	0.129	*VP*
	+4.4			*EP*	0.735	*G*	*EP*	0.708	*G*	*EP*	0.664	*F*
	+21.1			*PN*	0.614	*F*	*PN*	0.549	*F*	*PN*	0.487	*F*
	+37.8			*EP*	0.689	*F*	*EP*	0.622	*F*	*EP*	0.550	*F*
	+54.4			*PN*	0.735	*G*	*PN*	0.673	*F*	*PN*	0.618	*F*
5.0	−10.0	0.83	+50.0	*EP*	0.112	*VP*	*EP*	0.086	*VP*	*EP*	0.058	*VP*
	+4.4			*PN*	0.630	*F*	*PN*	0.566	*F*	*PN*	0.508	*F*
	+21.1			*PN*	0.705	*G*	*PN*	0.636	*F*	*PN*	0.572	*F*
	+37.8			*EP*	0.667	*F*	*EP*	0.602	*F*	*EP*	0.533	*F*
	+54.4			*EP*	0.641	*F*	*EP*	0.566	*F*	*PN*	0.499	*F*
10.0	−10.0	0.83	+50.0	*EP*	0.086	*VP*	*EP*	0.072	*VP*	*EP*	0.053	*VP*
	+4.4			*PN*	0.633	*F*	*PN*	0.565	*F*	*PN*	0.504	*F*
	+21.1			*PN*	0.739	*G*	*PN*	0.669	*F*	*PN*	0.605	*F*
	+37.8			*EP*	0.645	*F*	*EP*	0.583	*F*	*EP*	0.514	*F*
	+54.4			*EP*	0.661	*F*	*EP*	0.588	*F*	*EP*	0.515	*F*
25.0	−10.0	0.83	+50.0	*EP*	0.101	*VP*	*EP*	0.081	*VP*	*EP*	0.058	*VP*
	+4.4			*PN*	0.608	*F*	*PN*	0.536	*F*	*PN*	0.474	*F*
	+21.1			*PN*	0.750	*G*	*PN*	0.681	*F*	*PN*	0.618	*F*
	+37.8			*PN*	0.626	*F*	*PN*	0.557	*F*	*PN*	0.492	*F*
	+54.4			*EP*	0.626	*F*	*EP*	0.556	*F*	*EP*	0.485	*F*

Note: f – frequency; *T* – temperature; *BFL* – best-fit line; *CD* – co-efficient of determination; *GF* – goodness of fit; *EP* – exponential; *PN* – polynomial; *F* – fair; *E* – excellent; *G* – good; *P* – poor; *VP* – very poor.

addition, it was observed that the relationship was stronger for 10 000 wheel passes in the HWRT rutting test. The relationship was weaker for higher wheel passes (15 000 and 20 000); the coefficient of determination decreased in all cases when the HWRT wheel passes were greater than 10 000. This is due to a relatively low rutting rate in the plastic range of deformation. The deformation rate significantly decreased beyond 10 000 wheel passes (Table 6).

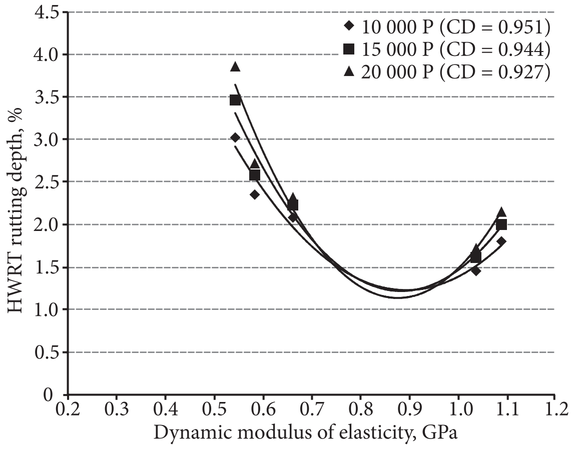

Fig. 1. Excellent relationships between dynamic modulus and HWRT rutting depth (f = 0.1 Hz, T = +54.4 °C)

The relationship between dynamic modulus and FLRT rutting depth was excellent for all FLRT load cycles when the loading frequencies and test temperature of the dynamic modulus test were 1.0–25.0 Hz and +46.1 °C, respectively (Figs 2–5). Among these excellent relationships, the highest strength of relationship was obtained for the loading frequency of 5.0 Hz (Fig. 3). At the same temperature (+46.1 °C) and 0.1–0.5 Hz loading frequencies, good to excellent relationships were also observed between dynamic modulus and FLRT rutting depth (Figs 6 and 7). Moreover, a good relationship was observed at 0.1 Hz and +37.8 °C for all FLRT load cycles (Fig. 8). The best-fit lines were primarily polynomial. The coefficient of determination for the relationships at 1.0–25.0 Hz and +46.1 °C varied in the range of 0.925–0.994 while it differed from 0.787 to 0.961 for the relationships at 0.1–0.5 Hz and +46.1 °C. The coefficient of determination varied in the range of 0.824–0.889 for the relationships at 0.1 Hz and +37.8 °C. The relationships were fair to good or very poor/poor to fair for the other cases of loading frequencies and test temperatures used in the dynamic modulus test (Table 10). In particular, the strength of

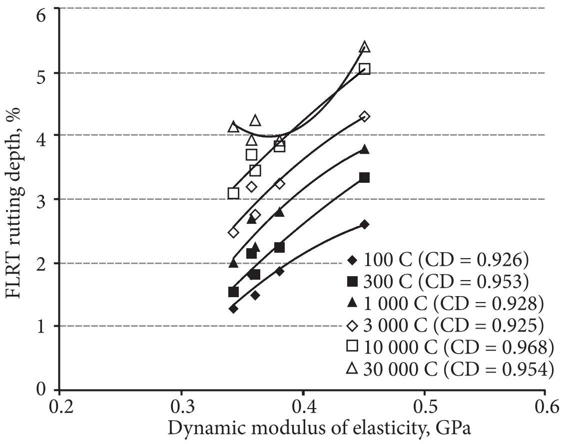

Fig. 2. Excellent relationships between dynamic modulus and FLRT rutting depth (f = 1.0 Hz, T = +46.1 °C)

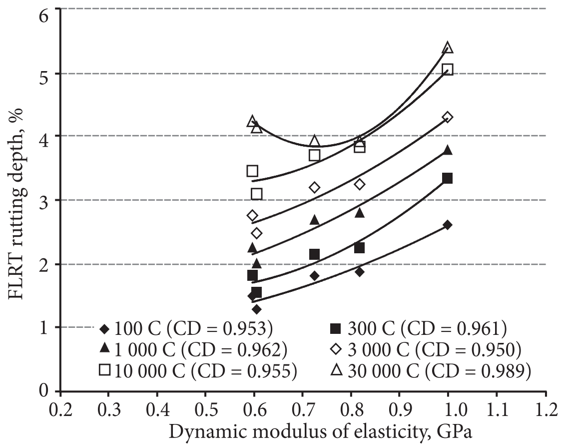

Fig. 4. Excellent relationships between dynamic modulus and FLRT rutting depth (f = 10.0 Hz, T = +46.1 °C)

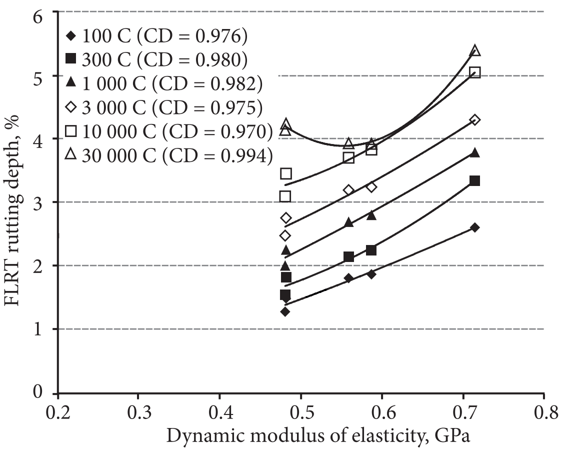

Fig. 3. Excellent relationships between dynamic modulus and FLRT rutting depth (f = 5.0 Hz, T = +46.1 °C)

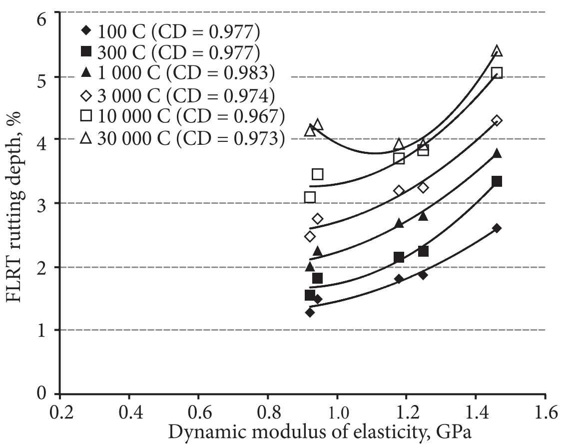

Fig. 5. Excellent relationships between dynamic modulus and FLRT rutting depth (f = 25.0 Hz, T = +46.1 °C)

Table 10. Relationship between stiffness and FLRT rutting depth

DM stiffness test conditions		FLRT rutting test conditions		Nature of relationship between DM and FLRT rutting depth																	
				100 cycles			300 cycles			1000 cycles			3000 cycles			10 000 cycles			30 000 cycles		
f, Hz	*T*, °C	*f*, Hz	*T*, °C	*BFL*	*CD*	*GF*	*BFL*	*CD*	*GF*	*BFL*	*CD*	*GF*	*BFL*	*CD*	*GF*	*BFL*	*CD*	*GF*	*BFL*	*CD*	*GF*
0.1	-10.0	1	+60.0	*PN*	0.838	*G*	*PN*	0.836	*G*	*PN*	0.851	*G*	*PN*	0.825	*G*	*PN*	0.834	*G*	*PN*	0.635	*F*
	+4.4			*EP*	0.683	*F*	*EP*	0.636	*F*	*EP*	0.695	*G*	*EP*	0.652	*F*	*EP*	0.570	*F*	*PN*	0.096	*VP*
	+21.1			*PN*	0.732	*G*	*PN*	0.678	*F*	*PN*	0.722	*G*	*PN*	0.733	*G*	*PN*	0.650	*F*	*PN*	0.475	*F*
	+37.8			*PN*	0.877	*G*	*PN*	0.884	*G*	*PN*	0.864	*G*	*PN*	0.889	*G*	*PN*	0.887	*G*	*PN*	0.824	*G*
	+46.1			*PN*	0.789	*G*	*PN*	0.848	*G*	*PN*	0.787	*G*	*PN*	0.806	*G*	*PN*	0.868	*G*	*PN*	0.961	*E*
0.5	-10.0	1	+60.0	*PN*	0.791	*G*	*PN*	0.779	*G*	*PN*	0.806	*G*	*PN*	0.775	*G*	*PN*	0.772	*G*	*PN*	0.515	*F*
	+4.4			*EP*	0.680	*F*	*EP*	0.632	*F*	*EP*	0.692	*F*	*EP*	0.650	*F*	*EP*	0.565	*F*	*PN*	0.093	*VP*
	+21.1			*PN*	0.677	*F*	*PN*	0.611	*F*	*PN*	0.672	*F*	*PN*	0.674	*F*	*PN*	0.569	*F*	*PN*	0.305	*P*
	+37.8			*EP*	0.766	*G*	*EP*	0.699	*G*	*EP*	0.751	*G*	*EP*	0.739	*G*	*EP*	0.623	*F*	*PN*	0.189	*VP*
	+46.1			*PN*	0.843	*G*	*PN*	0.895	*E*	*PN*	0.847	*G*	*PN*	0.849	*G*	*PN*	0.916	*E*	*PN*	0.940	*E*
1.0	-10.0	1	+60.0	*PN*	0.777	*G*	*PN*	0.975	*E*	*PN*	0.792	*G*	*PN*	0.760	*G*	*PN*	0.753	*G*	*PN*	0.480	*F*
	+4.4			*EP*	0.678	*F*	*EP*	0.630	*F*	*EP*	0.690	*F*	*EP*	0.648	*F*	*EP*	0.563	*F*	*PN*	0.095	*VP*
	+21.1			*PN*	0.669	*F*	*PN*	0.600	*F*	*PN*	0.666	*F*	*PN*	0.664	*F*	*PN*	0.555	*F*	*PN*	0.253	*P*
	+37.8			*PW*	0.697	*G*	*PW*	0.624	*F*	*PW*	0.689	*F*	*PW*	0.666	*F*	*PW*	0.539	*F*	*PN*	0.047	*VP*
	+46.1			*PN*	0.926	*E*	*PN*	0.953	*E*	*PN*	0.928	*E*	*PN*	0.925	*E*	*LG*	0.968	*E*	*PN*	0.954	*E*
5.0	-10.0	1	+60.0	*PN*	0.755	*G*	*PN*	0.738	*G*	*PN*	0.771	*G*	*PN*	0.738	*G*	*PN*	0.728	*G*	*PN*	0.442	*F*
	+4.4			*EP*	0.667	*F*	*EP*	0.619	*F*	*EP*	0.680	*F*	*EP*	0.638	*F*	*EP*	0.552	*F*	*PN*	0.092	*VP*
	+21.1			*EP*	0.602	*F*	*EP*	0.548	*F*	*EP*	0.613	*F*	*PW*	0.573	*F*	*EP*	0.477	*F*	*PN*	0.064	*VP*
	+37.8			*PW*	0.640	*F*	*PW*	0.571	*F*	*PW*	0.642	*F*	*PW*	0.608	*F*	*PW*	0.486	*F*	*PN*	0.104	*VP*
	+46.1			*PN*	0.976	*E*	*PN*	0.980	*E*	*PN*	0.982	*E*	*PN*	0.975	*E*	*PN*	0.970	*E*	*PN*	0.994	*E*
10.0	-10.0	1	+60.0	*PN*	0.746	*G*	*PN*	0.727	*G*	*PN*	0.762	*G*	*PN*	0.728	*G*	*PN*	0.717	*G*	*PN*	0.417	*F*
	+4.4			*EP*	0.678	*F*	*EP*	0.629	*F*	*EP*	0.690	*F*	*EP*	0.648	*F*	*EP*	0.560	*F*	*PN*	0.096	*VP*
	+21.1			*PN*	0.643	*F*	*PN*	0.568	*F*	*PN*	0.645	*F*	*PN*	0.633	*F*	*PN*	0.519	*F*	*PN*	0.140	*VP*
	+37.8			*PW*	0.611	*F*	*PW*	0.542	*F*	*PW*	0.615	*F*	*PW*	0.578	*F*	*PW*	0.459	*F*	*PN*	0.145	*VP*
	+46.1			*PN*	0.953	*E*	*PN*	0.961	*E*	*PN*	0.962	*E*	*PN*	0.950	*E*	*PN*	0.955	*E*	*PN*	0.989	*E*
25.0	-10.0	1	+60.0	*PN*	0.764	*G*	*PN*	0.749	*G*	*PN*	0.779	*G*	*PN*	0.747	*G*	*PN*	0.742	*G*	*PN*	0.464	*F*
	+4.4			*EP*	0.675	*F*	*EP*	0.626	*F*	*EP*	0.688	*F*	*EP*	0.646	*F*	*EP*	0.558	*F*	*PN*	0.099	*VP*
	+21.1			*PW*	0.642	*F*	*PW*	0.579	*F*	*PW*	0.648	*F*	*PN*	0.623	*F*	*PN*	0.509	*F*	*PN*	0.107	*VP*
	+37.8			*PW*	0.610	*F*	*PW*	0.542	*F*	*PW*	0.614	*F*	*PW*	0.576	*F*	*PW*	0.459	*F*	*PN*	0.138	*VP*
	+46.1			*PN*	0.977	*E*	*PN*	0.977	*E*	*PN*	0.983	*E*	*PN*	0.974	*E*	*PN*	0.967	*E*	*PN*	0.973	*E*
RM stiffness test conditions		FLRT rutting test conditions		100 cycles			300 cycles			1000 cycles			3000 cycles			10 000 cycles			30 000 cycles		
f, Hz	*T*, °C	*f*, Hz	*T*, °C	*BFL*	*CD*	*GF*	*BFL*	*CD*	*GF*	*BFL*	*CD*	*GF*	*BFL*	*CD*	*GF*	*BFL*	*CD*	*GF*	*BFL*	*CD*	*GF*
1	+25.0	1	+60.0	*PW*	0.563	*F*	*PW*	0.499	*F*	*PW*	0.571	*F*	*PN*	0.545	*F*	*PN*	0.433	*F*	*PN*	0.140	*VP*

Note: f – frequency; *T* – temperature; *BFL* – best-fit line; *CD* – co-efficient of determination (R^2); *GF* – goodness of fit; *EP* – exponential; *LG* – logarithmic; *PN* – polynomial; *PW* – power; *F* – fair; *E* – excellent; *G* – good; *P* – poor; *VP* – very poor.

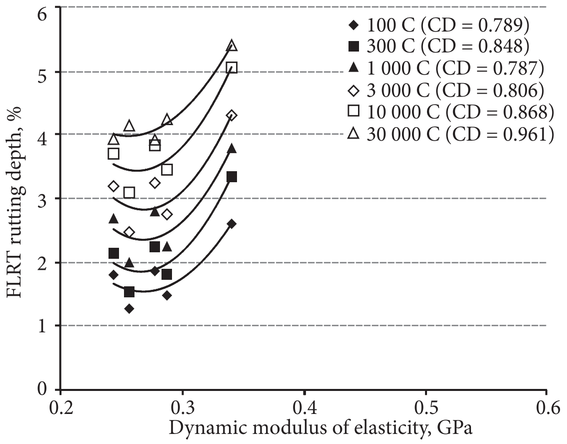

Fig. 6. Good to excellent relationships between dynamic modulus and FLRT rutting depth (f = 0.1 Hz, T = +46.1 °C)

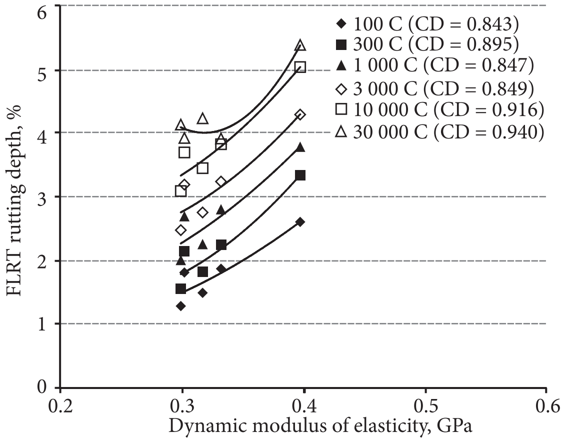

Fig. 7. Good to excellent relationships between dynamic modulus and FLRT rutting depth (f = 0.5 Hz, T = +46.1 °C)

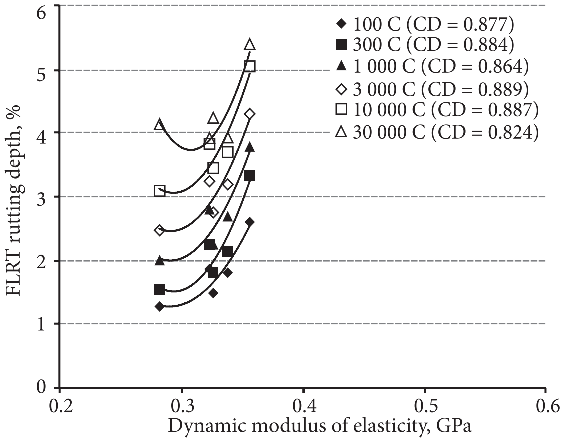

Fig. 8. Good relationships between dynamic modulus and FLRT rutting depth (f = 0.1 Hz, T = +37.8 °C)

relationships significantly decreased for 30 000 FLRT load cycles. This is because the rutting rate substantially decreased beyond 10 000 cycles. A similar trend was also observed in the case of HWRT rutting.

The FLRT rutting depth exhibited a stronger relationship with the dynamic modulus, as compared to the HWRT rutting depth. In particular, the FLRT rutting depth showed excellent relationships at 1.0–25.0 Hz, and good to excellent relationships at 0.1 and 0.5 Hz for the testing temperature of +46.1 °C. It was also observed that the fair to good relationships mostly exist between dynamic modulus and the FLRT rutting depth for all loading frequencies at –10.0 °C, which is in contrast with the outcomes of the HWRT rutting test. These findings imply that the FLRT test is more reliable than the HWRT test. This is possibly because the load used in FLRT rutting test was more representative of the real traffic conditions. However, similar to the HWRT rutting depth, the FLRT rutting depth in many cases of the load cycles greater than 10 000 showed very poor to poor relationships with the dynamic modulus (Table 10).

The trend lines for the relationship between dynamic modulus and HWRT/FLRT rutting depth varied depending on the loading frequency and testing temperature. In many cases, the trend line reversed. For example, the best-fit trend line in the case of HWRT rutting depth reversed at 0.1 Hz (the lowest loading frequency) and +54.4 °C (the highest temperature) after a certain limit of dynamic modulus (Fig. 1). A similar tendency was also noticed in the case of FLRT rutting depth at 0.1 Hz (the lowest loading frequency) and +46.1 °C (the highest temperature) (Fig. 6). Pellinen and Witczak (2002) reported that the correlation between dynamic modulus and rutting depth reverses at lower loading frequencies. In the present study, the trend line also reversed after a lower level of rutting depth when the loading was 30 000 cycles in many cases of the FLRT rutting test (Figs 2–8). This suggests that the loading range used in rutting test also influences the relationship between dynamic modulus and rutting depth.

4.5. Relationship between resilient modulus and rutting depth

The resilient modulus values were obtained for the asphalt Mixes 6–10, which were also tested for the rutting resistance by the FLRT test. For these asphalt mixes, the relationship between the resilient modulus and the FLRT rutting depth was examined. The goodness of the relationship was determined using the criteria shown in Table 8. The characteristics of the best-fit relationship are given in Table 10. The type of the best-fit line was power at lower FLRT load cycles but polynomial at higher load cycles. The relationship was fair up to 10 000 load cycles with a coefficient of determination significantly below 0.70. At 30 000 load cycles, the relationship was very poor. Both the resilient modulus and FLRT rutting tests were conducted at the loading frequency of 1 Hz. However, the test temperature was +25.0 °C for the resilient modulus and +60.0 °C for the FLRT rutting depth. The relationship between resilient modulus and FLRT rutting depth was not good due to such significantly differing test temperatures.

5. Conclusions

The relationship between the stiffness and rutting resistance of hot-mix asphalt mixes was emphasized in the present study. The stiffness was determined with respect to resilient and dynamic moduli. The rutting resistance was evaluated with regard to rutting depth obtained from the Hamburg Wheel Rut Tester and the French Laboratory Rutting Tester. The relationships of dynamic and resilient moduli with rutting depth were examined based on the regression analysis. The following conclusions are drawn from the findings of the present study.

1. All hot-mix asphalt mixes had good rutting resistance, except for conventional mix HL3 (Mix 1). The rutting depth of the hot-mix asphalt Mixes 2–10 was significantly below the max allowable limit. In general, the rutting resistance of the hot-mix asphalt mixes showed good/excellent correlations with their stiffness for specific test conditions.

2. The relationship between dynamic modulus and Hamburg Wheel Rut Tester rutting depth of the asphalt mixes varied due to the different loading frequencies and temperatures used in the dynamic modulus test. The excellent relationship was obtained at 0.1 Hz and +54.4 °C. At +54.4 °C, good relationship was also observed for 0.5 Hz up to 15 000 wheel passes. Such good and excellent relationships were observed as the dynamic modulus test temperature and the Hamburg Wheel Rut Tester rutting test temperature were very close. In these cases, the dynamic modulus test temperature was +54.4 °C whereas the Hamburg Wheel Rut Tester rutting test temperature was +50.0 °C.

3. The relationship between the dynamic modulus and the French Laboratory Rutting Tester rutting depth of the asphalt mixes also differed because of the different loading frequencies and temperatures of the dynamic modulus test. The excellent relationship was observed at +46.1 °C for the loading frequencies of 1.0 Hz, 5.0 Hz, 10.0 Hz, and 25.0 Hz. Good to excellent relationships were also observed for the loading frequencies of 0.10 Hz and 0.50 Hz at +46.1 °C. Indeed, the relationship peaked at +46.1 °C in all cases of loading frequency. This is because the dynamic modulus test temperature of +46.1 °C was very close to that of the French Laboratory Rutting Tester rutting test.

4. The relationship between the dynamic modulus and the French Laboratory Rutting Tester rutting depth was influenced by the loading cycles used in rutting test. The trend line reversed after a lower level of rutting depth when the loading was 30 000 cycles.

5. The relationship of the dynamic modulus with both the French Laboratory Rutting Tester rutting depth and the Hamburg Wheel Rut Tester rutting depth was very poor to poor in many cases after 10 000 wheel passes or load cycles. This is due to a relatively small deformation in rutting tests that occurred in the plastic range of deformation.

6. The dynamic modulus showed a stronger relationship with the French Laboratory Rutting Tester rutting depth than the Hamburg Wheel Rut Tester rutting depth. Excellent relationships were observed between the dynamic modulus and the French Laboratory Rutting Tester rutting depth at 1.0–25.0 Hz and +46.1 °C; good to excellent relationships were also noticed for 0.1 Hz and 0.5 Hz at +46.1 °C.

7. There was no good relationship between the resilient modulus and the French Laboratory Rutting Tester rutting depth of the asphalt mixes. This is because the resilient modulus test and the French Laboratory Rutting Tester rutting test were conducted at significantly different temperatures.

8. The dynamic modulus obtained at 0.1–1.0 Hz and +46.1 °C–(+54.4) °C are recommended to predict the rutting resistance of hot-mix asphalt mixes.

Acknowledgements

The authors express sincere gratitude to Miller Paving Limited and Ontario Centres of Excellence for Materials and Manufacturing for their cooperation in accomplishing the research project. The authors are also grateful to Golder Associates Limited for the technical support in conducting some of the tests carried out in the research project.

References

Ahmad, J.; Rahman, M. Y. A.; Hainin, M. R. 2011. Rutting Evaluation of Dense Graded Hot Mix Asphalt Mixture, *International Journal of Engineering and Technology* 11(5): 56–60.

Al-Khateeb, G. G.; Khedaywi, T. S.; Al-Suleiman, T. I.; Najib, A. M. 2013. Laboratory Study for Comparing Rutting Performance of Limestone and Basalt Superpave Asphalt Mixtures, *Journal of Materials in Civil Engineering* 25(1): 21–29. http://dx.doi.org/10.1061/(ASCE)MT.1943-5533.0000519

Al-Suhaibani, A.; Al-Mudaiheem, J.; Al-Fozan, F. 1992. Effect of Filler Type and Content on Properties of Asphalt Concrete Mixes, in *Effects of Aggregates and Mineral Fillers on Asphalt Mixture Performance.* ASTM STP 1147, American Society for Testing and Materials (ASTM), Philadelphia, USA, 107–130.

Bhattacharjee, S.; Mallick, R. B.; Daniel, J. S. 2008. Effect of Loading and Temperature on Dynamic Modulus of Hot Mix Asphalt Tested under MMLS3, *Airfield and Highway Pavements,* American Society of Civil Engineers (ASCE), Virginia, USA. 267–278.

Coleri, E.; Harvey, J. T.; Yang, K.; Boone, J. M. 2013. Micromechanical Investigation of Open-Graded Asphalt Friction Courses' Rutting Mechanisms, *Construction and Building Materials* 44: 25–34. http://dx.doi.org/10.1016/j.conbuildmat.2013.03.027

Čygas, D.; Mučinis, D.; Sivilevičius, H.; Abukauskas, N. 2011. Dependence of the Recycled Asphalt Mixture Physical and Mechanical Properties on the Grade and Amount of Rejuvenating Bitumen, *The Baltic Journal of Road and Bridge Engineering* 6(2): 124–134. http://dx.doi.org/10.3846/bjrbe.2011.17

Blazejowski, K.; Dolzycki, B. 2014. Relationships between Asphalt Mix Rutting Resistance and MSCR Test Results, in *Design, Analysis, and Asphalt Material Characterization for Road and Airfield Pavements,* American Society of Civil Engineers (ASCE), Virginia, USA. 202–209. http://dx.doi.org/10.1061/9780784478462.025

Erlingsson, S. 2012. Rutting Development in a Flexible Pavement Structure, *Road Materials and Pavement Design* 13(2): 218–234. http://dx.doi.org/10.1080/14680629.2012.682383

Goh, S. W.; You, Z.; Williams, R. C.; Li, X. 2011. Preliminary Dynamic Modulus Criteria of HMA for Field Rutting of Asphalt Pavements: Michigan's Experience, *Journal of Transportation Engineering* 137(1): 37–45. http://dx.doi.org/10.1061/(ASCE)TE.1943-5436.0000191

Hu, S.; Zhou, F.; Scullion, T. 2011. Development, Calibration, and Validation of a New M-E Rutting Model for HMA Overlay Design and Analysis, *Journal of Materials in Civil Engineering* 23(2): 89–99. http://dx.doi.org/10.1061/(ASCE)MT.1943-5533.0000130

Khan, K. M.; Kamal, M. A. 2012. Rutting Based Evaluation of Asphalt Mixes, *Pakistan Journal of Engineering and Applied Sciences* 11: 60–65.

Khedr, S. A.; Breakah, T. M. 2011. Rutting Parameters of Asphalt Concrete for Different Asphalt Structures, *International Journal of Pavement Engineering* 12(1): 11–23. http://dx.doi.org/10.1080/10298430903578960

Loulizi, A.; Flintsch, G. W.; Al-Qadi, I. L.; Mokarem, D. 2006. Comparing Resilient Modulus and Dynamic Modulus of Hot-Mix Asphalt as Material Properties for Flexible Pavement Design, *Transportation Research Record* 1970: 161–170. http://dx.doi.org/10.3141/1970-19

Neubauer, O.; Partl, M. N. 2004. Impact of Binder Content on Selected Properties of Stone Mastic Asphalt, in *Proc. of the 3rd Eurasphalt and Eurobitume Congress*, vol. 2. May 12–14, 2004, Vienna, Austria. 1614–1621.

Pellinen, T. K.; Witczak, M. W. 2002. Use of Stiffness of Hot-Mix Asphalt as a Simple Performance Test, *Transportation Research Record* 1789: 80-90. http://dx.doi.org/10.3141/1789-09

Roy, N.; Veeraragavan, A.; Krishna, J. M. 2013. Influence of Air Voids of Hot Mix Asphalt on Rutting within the Framework of Mechanistic-Empirical Pavement Design, *Procedia – Social and Behavioral Sciences* 104(2): 99–108. http://dx.doi.org/10.1016/j.sbspro.2013.11.102

Sivilevičius, H.; Podvezko, V.; Vakrinienė, S. 2011. The Use of Constrained and Unconstrained Optimization Models in Gradation Design of Hot Mix Asphalt Mixture, *Construction and Building Materials* 25(1): 115–122. http://dx.doi.org/10.1016/j.conbuildmat.2010.06.050

Swamy, A. K.; Mitchell, L. F.; Hall, S. J.; Daniel, J. S. 2011. Impact of RAP on the Volumetric, Stiffness, Strength, and Low-Temperature Properties of HMA, *Journal of Materials in Civil Engineering* 23(11): 1490–1497. http://dx.doi.org/10.1061/(ASCE)MT.1943-5533.0000245

Tighe, S. L.; Jeffray, A.; Perraton, D. 2007. *Low Temperature Evaluation of Recycled Asphalt Shingles (RAS) into Base Course Asphalt Mixes*. Research Report (Prepared for Miller Paving Limited and Ontario Centres of Excellence for Materials and Manufacturing). University of Waterloo, Waterloo, Ontario, Canada.

Tran, N. H.; Hall, K. C. 2005. Evaluating the Predictive Equation in Determining Dynamic Modulus of Typical Asphalt Mixtures Used in Arkansas, *Journal of the Association of Asphalt Paving Technologists* 74: 1–17.

Uzarowski, L.; Tighe, S. L.; Rothenburg, L. 2008. Developing Rutting Criteria to Improve Safety Using the SPT, Hamburg Rut Tester and Modelling for Canadian Asphalt Mixes, in *Proc. of ISAP Conference 2008*. August 18–20, 2008, Zurich, Switzerland.

Uzarowski, L.; Maher, M.; Prilesky, H.; Tighe, S. L.; Rothenburg, L. 2006. The Use of Dynamic Modulus and Creep Tests in the Development of Rutting Resistant Criteria for Asphalt Mixes in Canada – Stage 1, in *Proc. of the 10th International Conference on Asphalt Pavements*. August 12–17, 2006, Quebec, Canada.

Uzarowski, L. 2006. *The Development of Asphalt Mix Creep Parameters and Finite Element Modeling of Rutting*. PhD thesis. University of Waterloo, Canada.

Uzarowski, L.; Paradis, M.; Lum, P. 2004. Accelerated Performance Testing of Canadian Asphalt Mixes Using Three Different Wheel Rut Testers, in *Proc. of the 2004 Annual Conference of the Transportation Association of Canada*, Quebec City, Quebec, Canada.

Yu, H.; Shen, S. 2012. *An Investigation of Dynamic Modulus and Flow Number Properties of Asphalt Mixtures in Washington State*. Final Report No. TNW2012-02, Washington State Transportation Center (TRAC), Washington State University, Washington DC, USA.

Received 11 June 2012; accepted 26 October 2012